

JH Green

Preliminary Results of Turbine Missile Casing Tests

EPRI

Project 399
Preliminary Report
October 1978

Prepared by
Sandia Laboratories
Albuquerque, New Mexico

ELECTRIC POWER RESEARCH INSTITUTE

7902020068

79020200

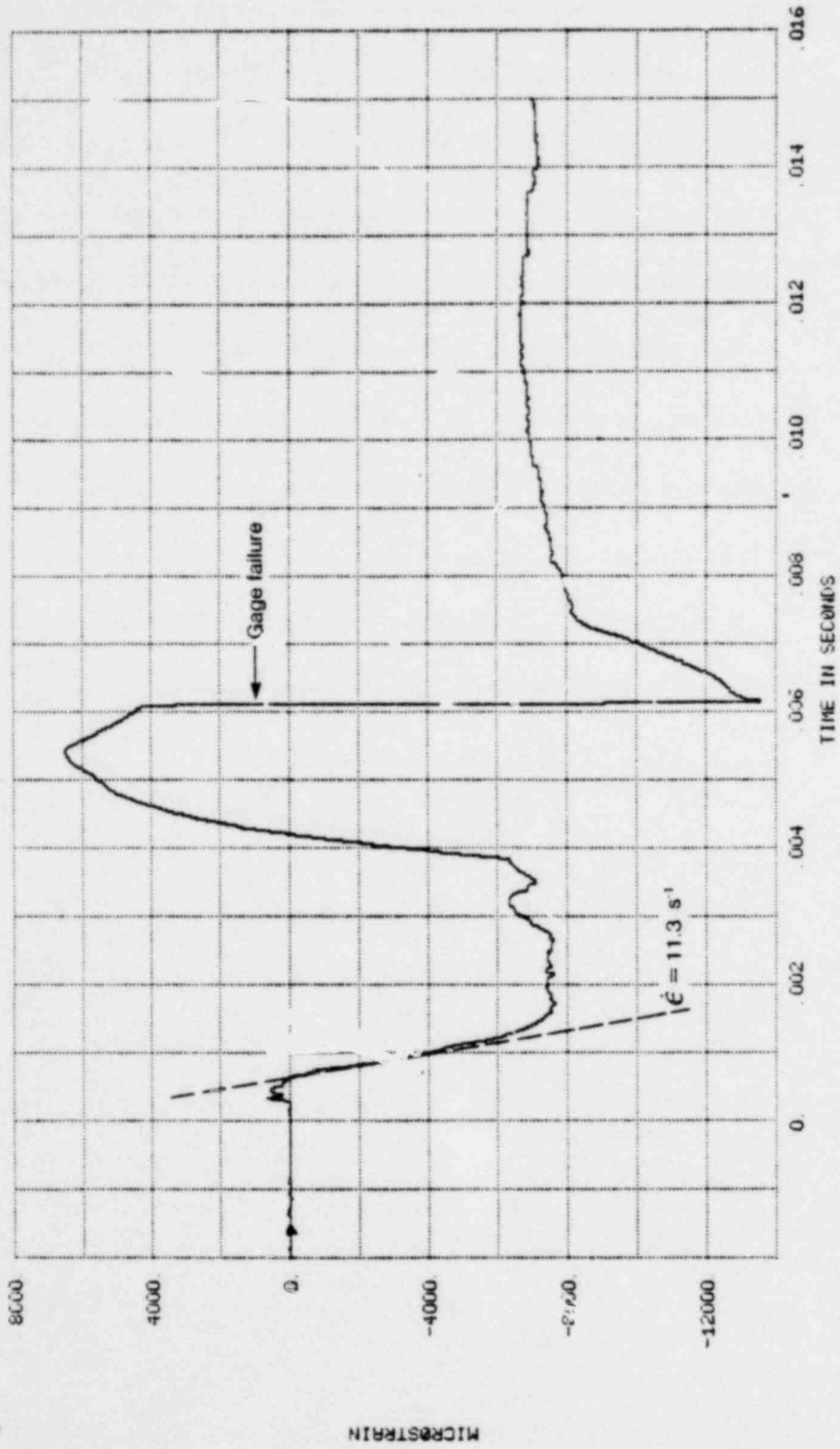


Figure 2-7. Strain record near impact point, blunt orientation (negative sign denotes tensile strain).

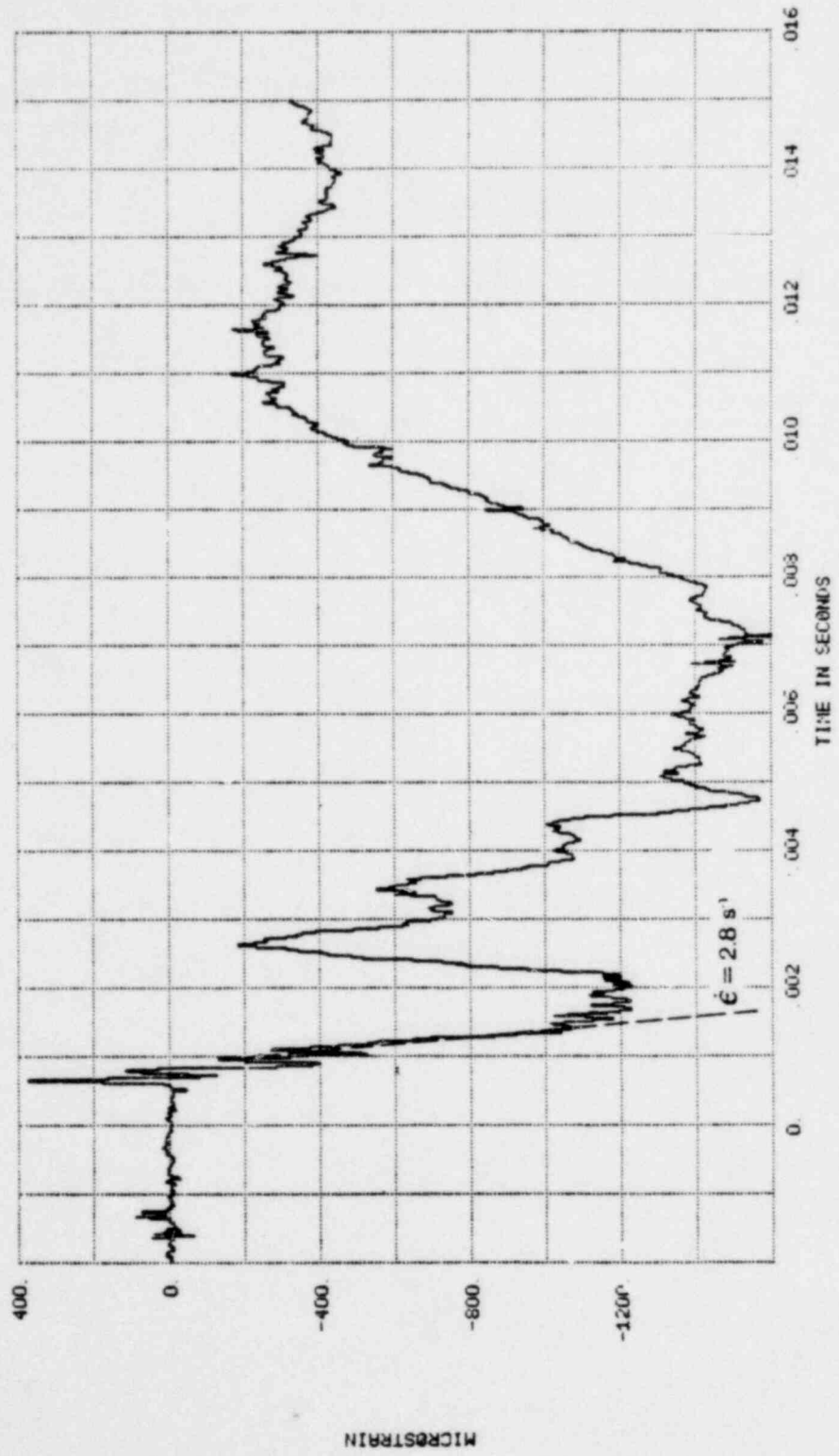


Figure 2-8. Strain record near support, blunt orientation (negative sign denotes tensile strain).

**Preliminary Results of
Turbine Missile Casing Tests**

Research Project 399

Preliminary Report, October 1978

Tests conducted by

SANDIA LABORATORIES
Albuquerque, New Mexico

Principal Investigators
H. Richard Yoshimura
John T. Schamaun

Tests conducted for

Electric Power Research Institute
3412 Hillview Avenue
Palo Alto, California 94304

EPRI Project Manager
George Sliter
Nuclear Power Division

EPRI PERSPECTIVE

PROJECT DESCRIPTION

This report presents preliminary results from initial tests in EPRI's turbine missile program. A detailed final report is scheduled for publication in early 1979. Extensive instrumentation recorded the response of two full-scale, simplified models of an 1800-rpm steam turbine casing, each impacted by a missile representing a fragment from a postulated failure of a shrunk-on disk. A rocket sled was used to launch the 1527-kg (3366-lb) missiles to impact the target ring and shell structure at 150 m/s (492 ft/s).

PROJECT OBJECTIVE

The objective was to provide benchmark data on both the energy-absorbing mechanisms of the impact process and, if breakthrough occurred, the exit conditions of the fragment. The data can be used in assessing the conservatism in present estimates of design exit velocities and in validating improved design and analysis methods.

CONCLUSIONS AND RECOMMENDATIONS

The tests showed that turbine casings can absorb substantial amounts of energy in slowing down or containing fragments from a postulated turbine failure. Additional testing and analysis are needed to quantify the energy that can be dissipated over a wider range of potential impact conditions. It is especially desirable to examine the effects of missile rotation upon impact. One of the tests showed that even though the missile was not rotating before impact, it was rotating after exiting the simulated casing. This rotation suggests that subsequent impacts on concrete structures that protect safety-related plant equipment are likely to be off-normal and not as severe as the nonspinning, normal-impact condition often assumed for turbine missile design. This reduced severity would be similar to that demonstrated by an off-normal impact of a steel pipe in the tornado missile program (EPRI NP-440).

A follow-on test series is under way to examine turbine missile impacts of full-scale concrete structures. Testing will be conducted in 1979.

George Sliter, Project Manager
Nuclear Power Division

ABSTRACT

Preliminary results are presented from two full-scale tests simulating the impact of turbine disk fragments on simple ring and shell structures that represent the internal stator blade ring and the outer wall of an 1800-rpm steam turbine casing. The objective is to provide benchmark data on both the energy-absorbing mechanisms of the impact process and, if breakthrough occurs, the exit conditions of the turbine missile. A rocket sled is used to accelerate a 1527-kg (3366-lb) segment of a turbine disk, which impacts a steel ring 12.7 cm (5 in) thick and a steel shell 3.2 cm (1.25 in) thick. The impact velocity of about 150 m/s (492 ft/s) gives a missile kinetic energy corresponding to the energy of a fragment from a postulated failure at the design overspeed. Depending on the orientation of the missile at impact, the steel test structure either slowed the missile to 60% of its initial translational velocity with an exit rotational speed of 115 rpm, or brought it almost to rest (an energy reduction of 65 and 100%, respectively). The report includes missile velocity histories and selected strain gage data. Detailed results will be included in the final report, now in preparation.

CONTENTS

<u>Section</u>		<u>Page</u>
1	TEST DESCRIPTION	1-1
2	TEST RESULTS	2-1

ILLUSTRATIONS

<u>Figure</u>	<u>Page</u>
1-1 Target structure, missile, and impact orientations.	1-4
1-2 Dimensions and mass properties of steel missile segment (120° hub section).	1-5
1-3 Missile, support sled, and rocket pusher sled.	1-6
2-1a Overhead photograph of piercing impact (V = 149 m/s, 490 ft/s; $\omega = 0$).	2-4
2-1b Overhead photograph of piercing impact (V = 99 m/s, 325 ft/s).	2-5
2-1c Overhead photograph of piercing impact (V = 87 m/s, 285 ft/s; $\omega = 115$ rpm).	2-6
2-2 Displacement history of missile in test with piercing orientation.	2-7
2-3 Strain record near impact point, piercing orientation.	2-8
2-4 Strain record near support, piercing orientation.	2-9
2-5a Overhead photograph of blunt impact (V = 151 m/s, 495 ft/s; $\omega = 0$).	2-10
2-5b Overhead photograph of blunt impact (V = 32 m/s, 105 ft/s).	2-11
2-5c Overhead photograph of blunt impact (V = 8 m/s, 25 ft/s; $\omega \approx 0$).	2-12
2-6 Displacement history of missile in test with blunt orientation.	2-13
2-7 Strain record near impact point, blunt orientation.	2-14
2-8 Strain record near support, blunt orientation.	2-15

TABLES

<u>Table</u>		<u>Page</u>
2-1	Missile Energy, Piercing Orientation	2-1
2-2	Missile Energy, Blunt Orientation	2-3

SUMMARY

Two full-scale rocket sled tests have been conducted to provide benchmark data for making more realistic assessments of turbine missile effects in nuclear plant design. The tests simulated the impact of a fragment from a failed shrunk-on turbine disk on the internal stator blade ring and the outer wall of an 1800-rpm low-pressure casing. High-speed photography and strain gages were used to measure data on both the energy-absorbing mechanisms of the impact process and, if breakthrough occurred, the exit velocity and rotation of the fragment.

In both tests the target structure was a simplified representation of a casing. Only the two main semicircular casing components that are expected to absorb most of the energy in a postulated failure were modeled: the internal blade ring or diaphragm, which supports the stationary turbine blades, represented by a steel ring 12.7 cm (5 in) thick; and the outer casing cover, represented by a steel shell 3.2 cm (1.25 cm) thick.

The ring and the shell were bolted to a massive reinforced-concrete backup structure. The bolted connections simulated as closely as practicable the horizontal joints in an actual turbine.

The missile in both tests was a 120° segment of a last-stage, shrunk-on disk weighing 1527 kg (3366 lb). The segment had no blades; it was assumed that the blades would be broken off or crushed during exit.

The nominal impact velocity in both tests was 146 m/s (480 ft/s), which gives the same total kinetic energy as a segment leaving a shaft spinning at 120% of operating speed. Since the orientation of a turbine segment at impact with the inner ring cannot be specified with certainty and since orientation has a great influence on absorbed energy, the missiles in the two tests had "bounding" orientations. In one test a piercing orientation, with sharp corner impact and minimum projected area, gave a lower bound on absorbed energy. In the other test a blunt orientation, with curved edge impact and maximum projected area, gave an upper bound on absorbed energy.

In the test with a piercing orientation, perforation of both structures slowed the missile to 60% of its initial speed (two-thirds of the missile's energy was absorbed). The segment was rotating as it exited the target structure. Designers will be able to take advantage of such off-normal and spinning conditions when calculating the effects of potential missile impacts on concrete walls.

In the test with a blunt orientation, the missile did not perforate either structure and was brought almost to rest.

Data from the tests will be reduced, compared with the results of pretest calculations, and presented in a final report.

Section 1

TEST DESCRIPTION

Two full-scale turbine casing exit tests have been completed at the rocket sled facility of Sandia Laboratories, Albuquerque, New Mexico. The tests simulated the impact of a fragment from a failed shrunk-on turbine disk on the internal stator blade ring and outer wall of an 1800-rpm low-pressure casing. The objective was to provide benchmark data on both the energy-absorbing mechanisms of the impact process and, if breakthrough occurred, the exit conditions of the fragment.

Because of wide variations in turbine designs, postulated failure conditions, and missile exit scenarios, the list of potential test parameters was large. The bounding parameters for the two tests were selected to give a first-order simulation of prototypical conditions while maintaining the well-characterized conditions needed for generating benchmark data.

TARGET STRUCTURE

The target structure in both tests was the same (Figure 1-1). The inner structure, representing a last-stage stationary-blade support ring, was 12.7 cm (5 in) thick, 50.8 cm (20 in) wide, and 431.8 cm (170 in) in diameter. The outer shell, representing a casing cover, was 3.2 cm (1.25 in) thick, 182.9 cm (72 in) wide, and 635 cm (250 in) in diameter. The ring and the shell were fabricated from ASTM A515, Grade 65 cold-rolled steel with a tensile yield of 300 MPa (43.6 ksi), a tensile ultimate of 491 MPa (71.4 ksi), and an elongation of 26% at room temperature.

The ring and the shell were bolted to a massive concrete structure and soil overburden weighing 1633 metric tons (1800 tons). The bolted connections simulated as closely as practicable the horizontal joints in an actual turbine. Twelve bolts that were 3.8 cm (1.5 in) in diameter held down each end of the ring; these had an ultimate strength of 11.5 MN (2.6×10^6 lbf) and an active length of 25.4 cm (10 in). Fourteen bolts 2.54 cm (1 in) in diameter held down each end of the shell; these had an ultimate strength of 6.7 MN (1.5×10^6 lbf) and an active length of 15.2 cm (6 in). The bolts were fabricated from A490 steel.

The ring was maintained near 38°C (100°F), typical of the temperature in the last-stage region of an operating turbine. Standard Charpy-V specimens from the ring material gave a strength of 20 J (15 ft lbf) at 38°C.

MISSILE IMPACT CONDITIONS

The missile in both tests was a 120° sector of a last-stage shrunk-on disk manufactured by Westinghouse Corporation. (The missile was selected from among several turbine disk segments provided for the test program by Westinghouse and General Electric Company.) Dimensions and mass properties of the 1527-kg (3366-lb) missile are given in Figure 1-2. The missile was made from high-strength alloy steel (ultimate strength of 896 MPa or 130 ksi). Note that the turbine sector has no blades; it is assumed that the blades break off or are crushed during exit.

The missile was mounted on a lightweight support sled, which was pushed by a rocket sled (Figure 1-3). After the acceleration stage the rocket sled was braked, allowing the missile and support sled to coast toward the target. Activation of explosive bolts just before impact separated the missile from the support sled, which was diverted by a striker plate beneath the target structure. The missile then traveled in free flight before its 15.5-cm-wide (6.1-in) edge struck the center of the 50.8-cm-wide (20-in) ring.

As indicated in Figure 1-1, the flight path of the missile's center of gravity was offset 51.3 cm (20.2 in) from the centerline of the track and the structure. This simulated the trajectory of a turbine segment that leaves the shaft translating tangentially from a circle through the segment's center of gravity. The rotation of the segment, which would be at the rotational velocity of the turbine at failure, was not simulated in the tests. Instead, the total translational and rotational energy of the hypothetical turbine segment was included in the translational energy of the test missile.

The nominal impact velocity in both tests was 146 m/s (480 ft/s). This translational velocity gave the same total kinetic energy (16.4×10^6 J, or 12.1×10^6 ft lbf) as a segment leaving a shaft spinning at 2160 rpm, or 120% of operating speed (the so-called design overspeed condition).

Since the orientation of a turbine segment at impact with the inner casing ring cannot be specified with certainty and since orientation has a large influence on absorbed energy, the missiles in the two tests had "bounding" orientations

(Figure 1-1). In the first test a piercing orientation, with sharp corner impact and minimum projected area, gave a lower bound on absorbed energy. In the second test a blunt orientation, 90° to the first, with curved edge impact and maximum projected area, gave an upper bound on absorbed energy.

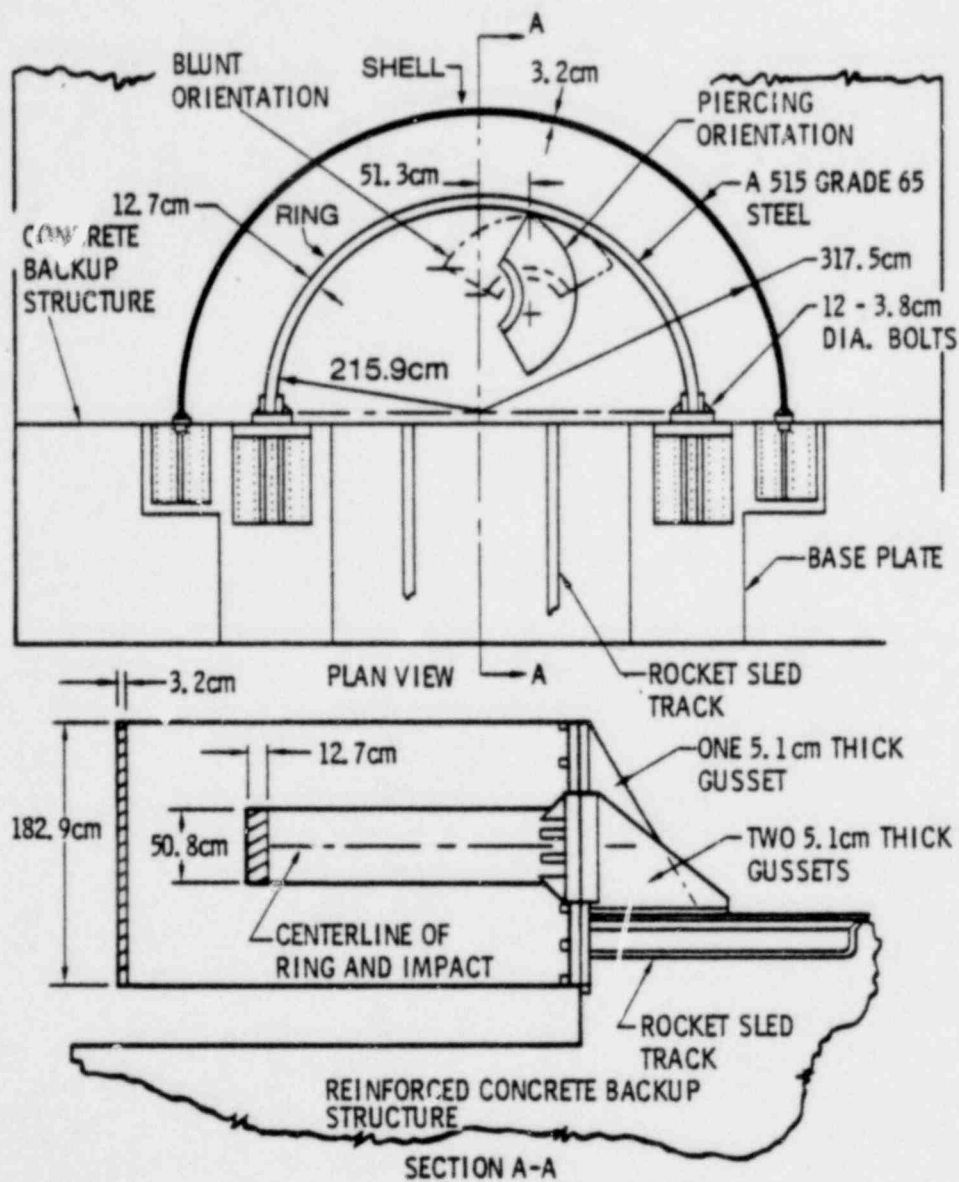
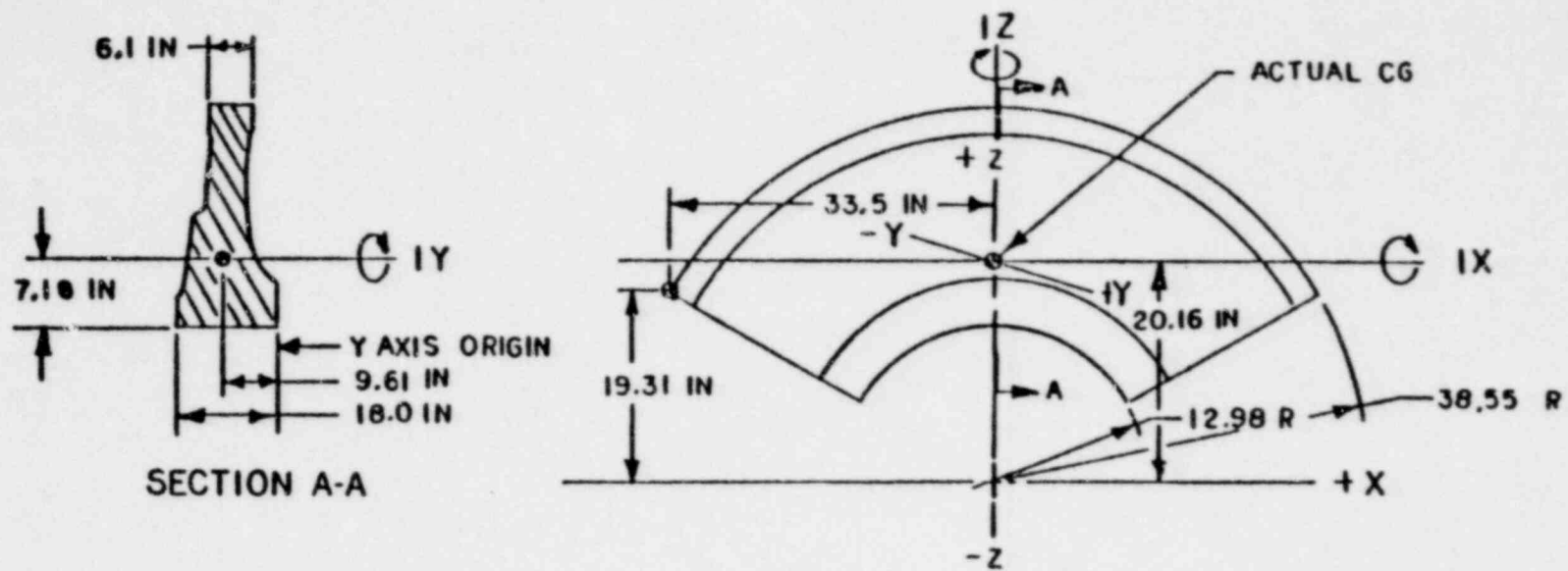


Figure 1-1. Target structure, missile, and impact orientations (1 cm = 0.3937 in).



Weight: 3365.8 lb
 Center of gravity: $X = 0$; $Y = -9.61$ in; $Z = 20.16$ in
 Mass moment of inertia:
 $I_X = 216783$ lb-in²
 $I_Y = 818410$ lb-in²
 $I_Z = 686254$ lb-in²

Figure 1-2. Dimensions and mass properties of steel missile segment (120° hub section) (1 in = 2.54 cm; 1 lb = 2.20 kg).

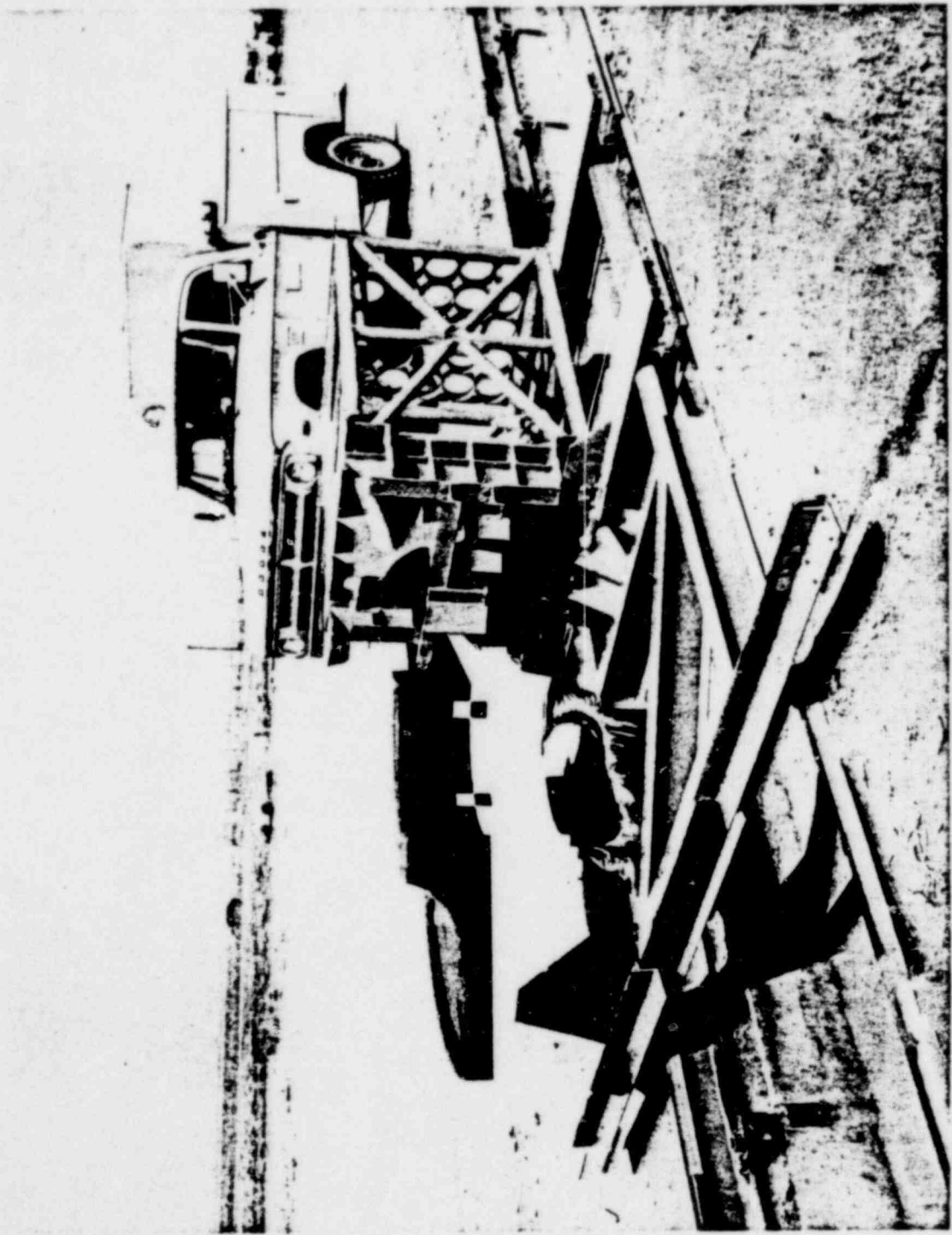


Figure 1-3. Missile, support sled, and rocket pusher sled.

Section 2
TEST RESULTS

In the test with a piercing orientation, the missile penetrated about 10 cm (4 in) into the ring, broke through both the ring and the shell, and exited with a translational velocity of 86.9 m/s (285 ft/s) (Figure 2-1a, b, c). After failure of the ring at the impact point, both ends of the ring broke at the edge of the welded gusset plates that connected the ring to its base plate. The bolts connecting the base plate to the backup structure did not fail.

A plot of missile displacement versus time taken from an overhead high-speed camera is shown in Figure 2-2, and missile velocity and energy at various times are summarized in Table 2-1. In slowing the missile to 58% of its initial speed, the structure absorbed two-thirds of the missile's energy; 85% of the absorbed energy was dissipated by ring impact and only 15% by shell impact.

Table 2-1
MISSILE ENERGY, PIERCING ORIENTATION

<u>Event</u>	<u>Time ms</u>	<u>Measured Velocity m/s (ft/s)</u>	<u>Kinetic Energy MJ (10⁶ ft·lbf)</u>	<u>Cumulative Energy Dissipation %</u>
Ring impact	0	149 (490)	17.0 (12.5)	0
Ring fracture to shell impact	2.5-9.5	99 (325)	7.5 (5.5)	56
After shell perforation	>20	87 (285)	5.7 (4.2)	66

The segment was rotating at 115 rpm after exiting the simulated casing (Figure 2-1c). The rotational energy imparted to the missile was negligible (0.6%) compared with the total exit energy. However, this rotation suggests that

an off-normal impact on a concrete target following exit is a more reasonable simulation of potential impact on buildings than the normal impact usually assumed for design.

The missile was only slightly deformed by the impact; the sharp corner was blunted about 1 in.

Samples of the records from 26 strain gages on the ring and the shell are given in Figures 2-3 and 2-4. The gage in Figure 2-3 measured circumferential membrane strain on the midsurface of the ring at a cross section through the impact point. A tensile strain of about 0.12% was measured before gage failure occurred within less than 1 ms (ring fracture occurred between 2.1 and 2.5 ms after impact). The maximum strain rate measured was $6 \times 10^6 \text{ s}^{-1}$. Strain rates are expected to be much higher at points closer to the impact area.

The gage in Figure 2-4 measured circumferential membrane strain at a cross section 12.1° from the support closest to the impact point. The strain peaked at about 2 ms after impact and began oscillating around a small residual strain at about 3 ms, when high-speed photography showed fracture at the nearby support. The peak reaction, estimated from strain measurements, was approximately 14.6 MN (3.3×10^6 lbf).

In the test with a blunt orientation, the missile did not perforate either the ring or the shell (Figure 2-5a, b, c). Instead the momentum transferred to the structures failed all of the support bolts, and the net energy dissipated brought the missile almost to rest. As indicated by the displacement, velocity, and energy histories in Figure 2-6 and Table 2, 95% of the missile's initial energy was dissipated as the ring impact slowed the missile to one-fifth of its initial speed. Missile velocity remained constant until impact with the shell absorbed virtually all of the remaining 5% of its energy.

Sample strain records are given in Figures 2-7 and 2-8. The gage in Figure 2-7 measured circumferential strain in the ring near the impact point (52° from the support). A peak strain of about 0.8% was measured before gage failure occurred at 6 ms.

Table 2-2
MISSILE ENERGY, BLUNT ORIENTATION

<u>Event</u>	<u>Time ms</u>	<u>Measured Velocity m/s (ft/s)</u>	<u>Kinetic Energy MJ (10⁶ ft·lbf)</u>	<u>Cumulative Energy Dissipation %</u>
Ring impact	0	151 (495)	17.4 (12.8)	0
Ring bolt failure to shell impact	9-18	32 (105)	0.8 (0.6)	95
Shell bolt failure	55	8 (25)	0.04 (0.03)	99.7

The gage in Figure 2-8 measured circumferential strain at a cross section 12.1° from the support closest to the impact point. The strain peaked at 7 ms after impact, which is the approximate time that high-speed photography showed bolt failure at the nearby support. The peak reaction, estimated from strain measurements, was approximately 19.0 MN (4.3×10^6 lbf).

Detailed data from both tests will be presented and compared with calculations in the final report. The report will include estimates of the amount of energy dissipated by various momentum transfer and energy absorption processes.

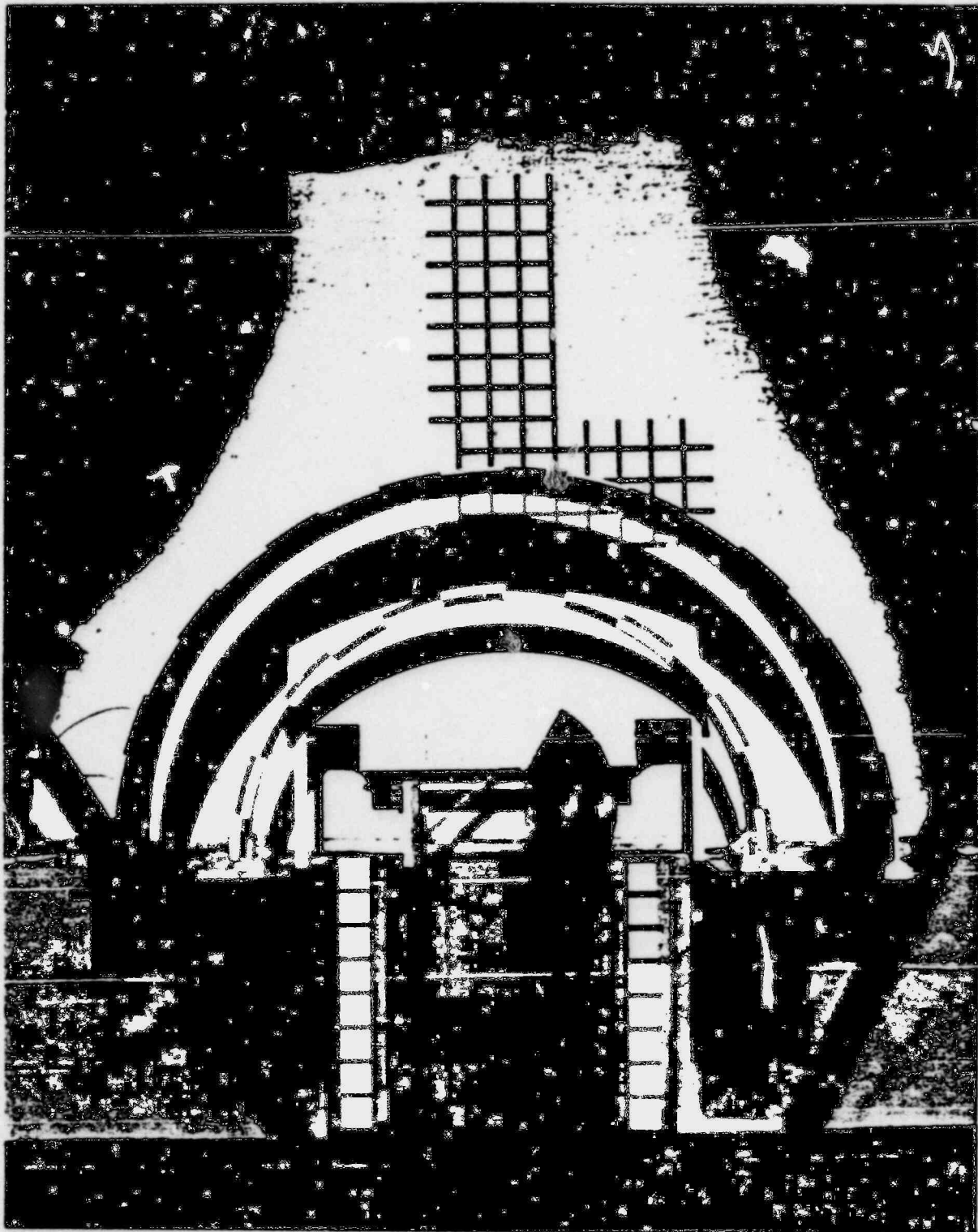


Figure 2-1a. Overhead photograph of piercing impact ($V = 149$ m/s, 490 ft/s; $\omega = 0$).

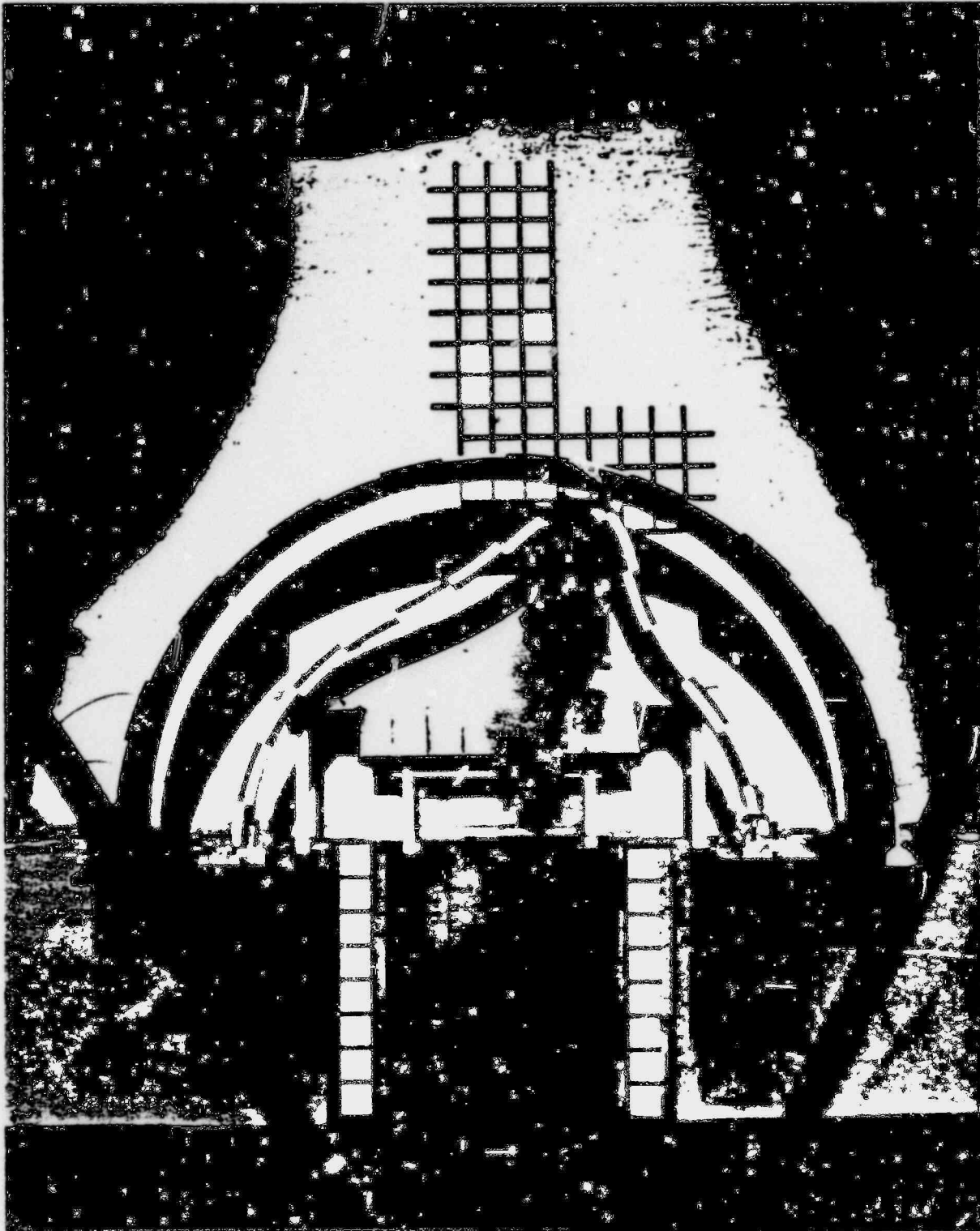


Figure 2-1b. Overhead photograph of piercing impact ($V = 99$ m/s, 325 ft/s).

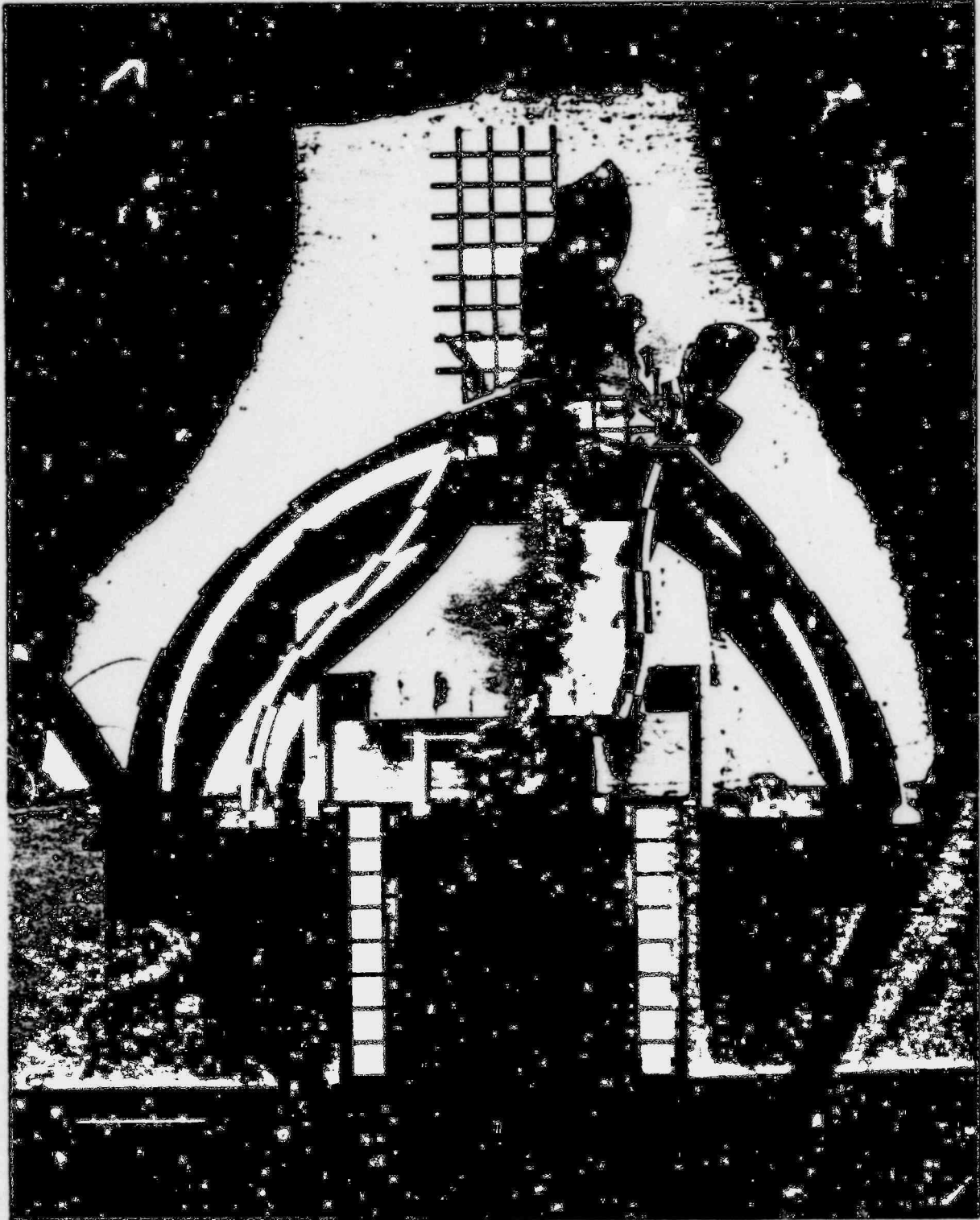


Figure 2-1c. Overhead photograph of piercing impact ($V = 87$ m/s, 285 ft/s; $\omega = 115$ rpm).

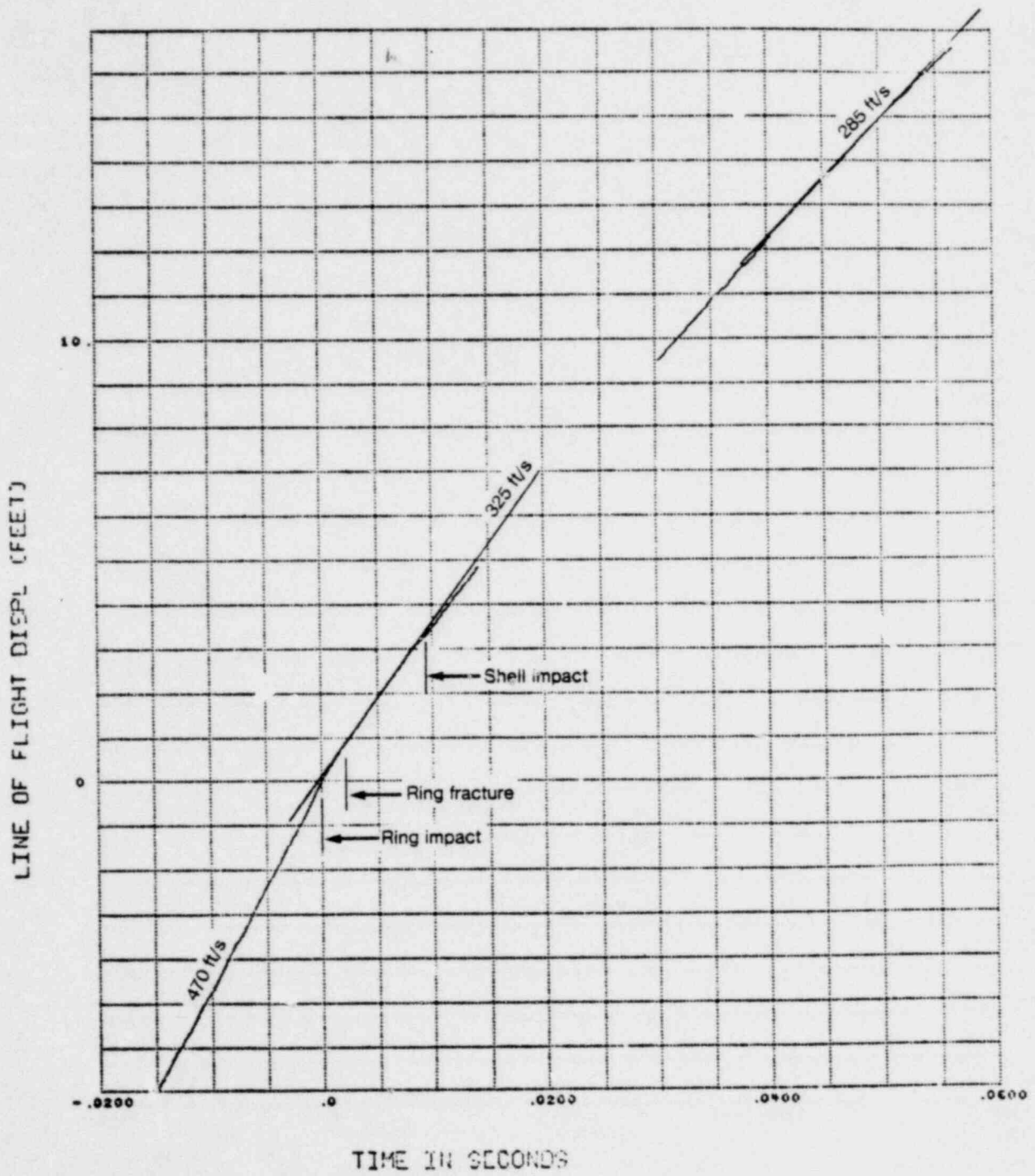


Figure 2-2. Displacement history of missile in test with piercing orientation
 (1 ft = 30.48 cm; 1 ft/s = 0.305 m/s)

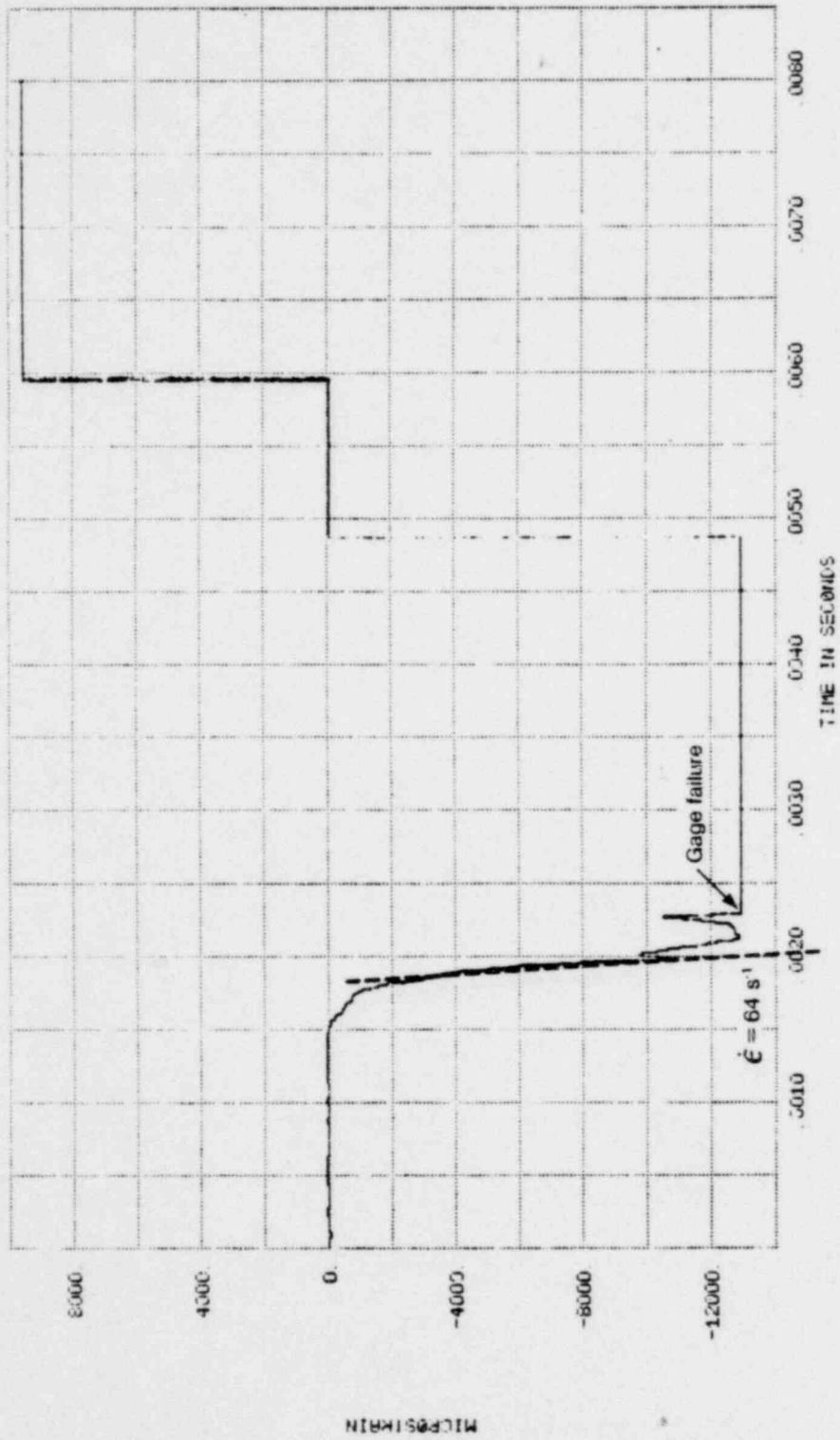


Figure 2-3. Strain record near impact point, piercing orientation (negative sign denotes tensile strain)

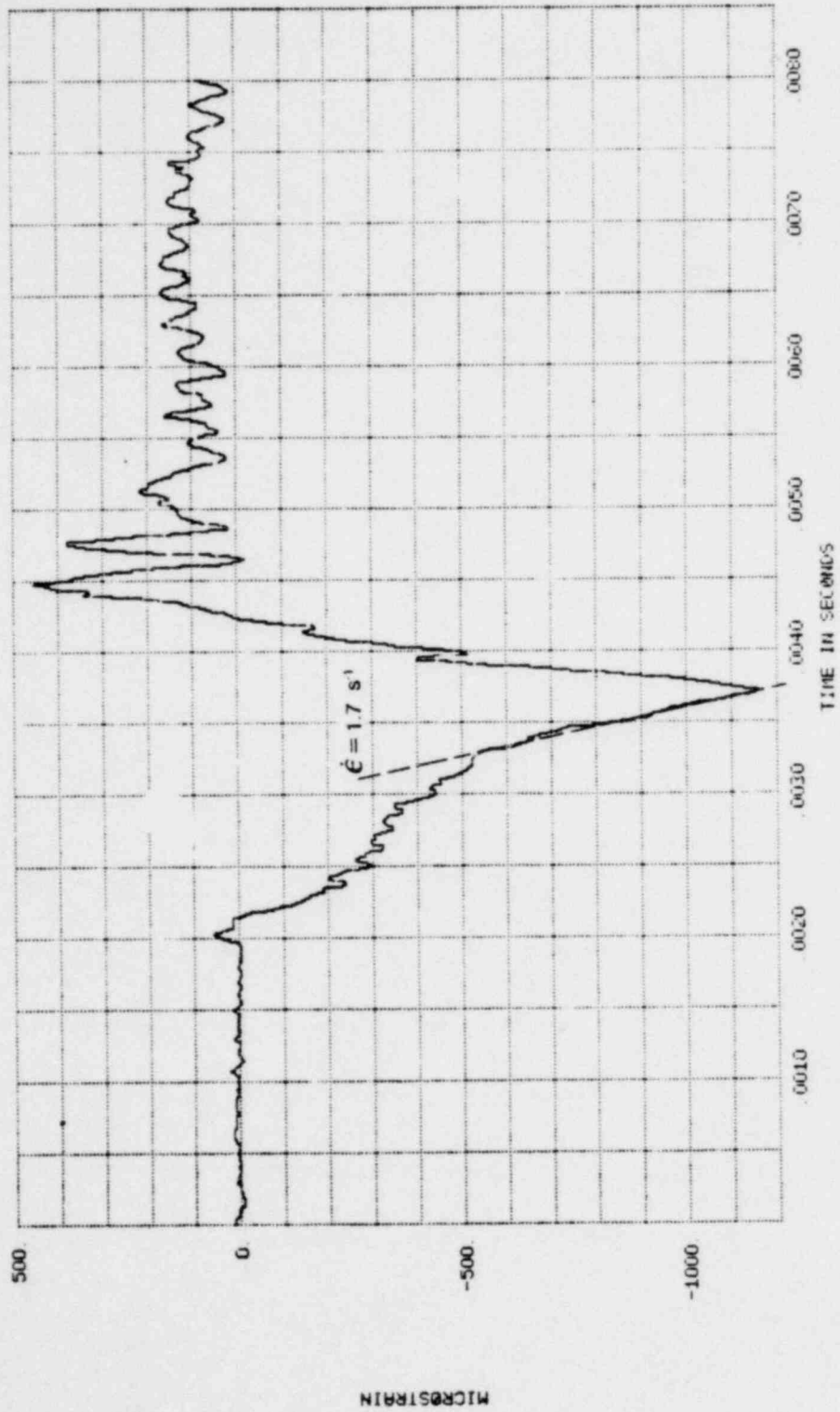


Figure 2-4. Strain record near support, piercing orientation (negative sign denotes tensile strain).

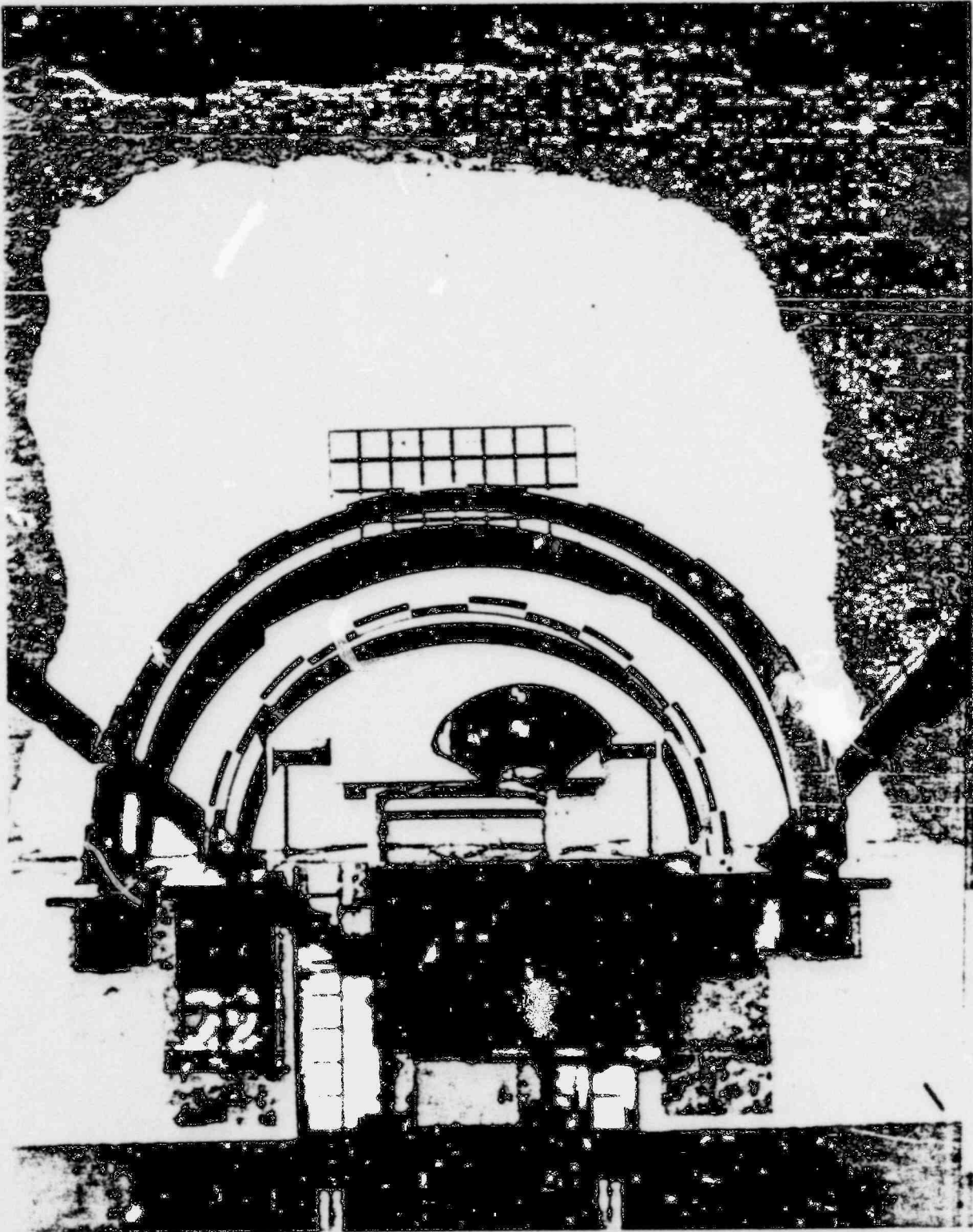


Figure 2-5a. Overhead photograph of blunt impact ($V = 151$ m/s, 495 ft/s; $\omega = 0$).

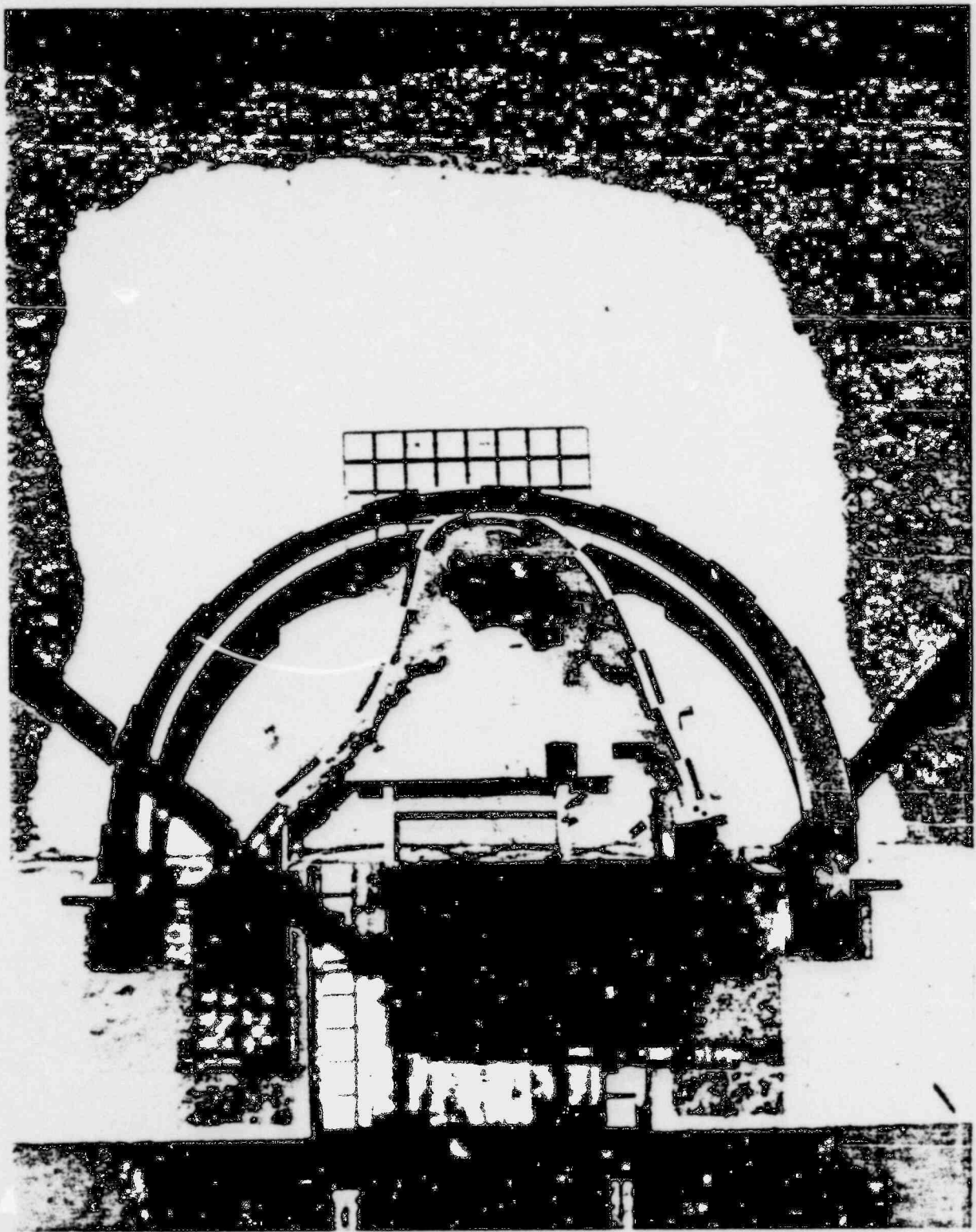


Figure 2-5b. Overhead photograph of blunt impact ($V = 32$ m/s, 105 ft/s).

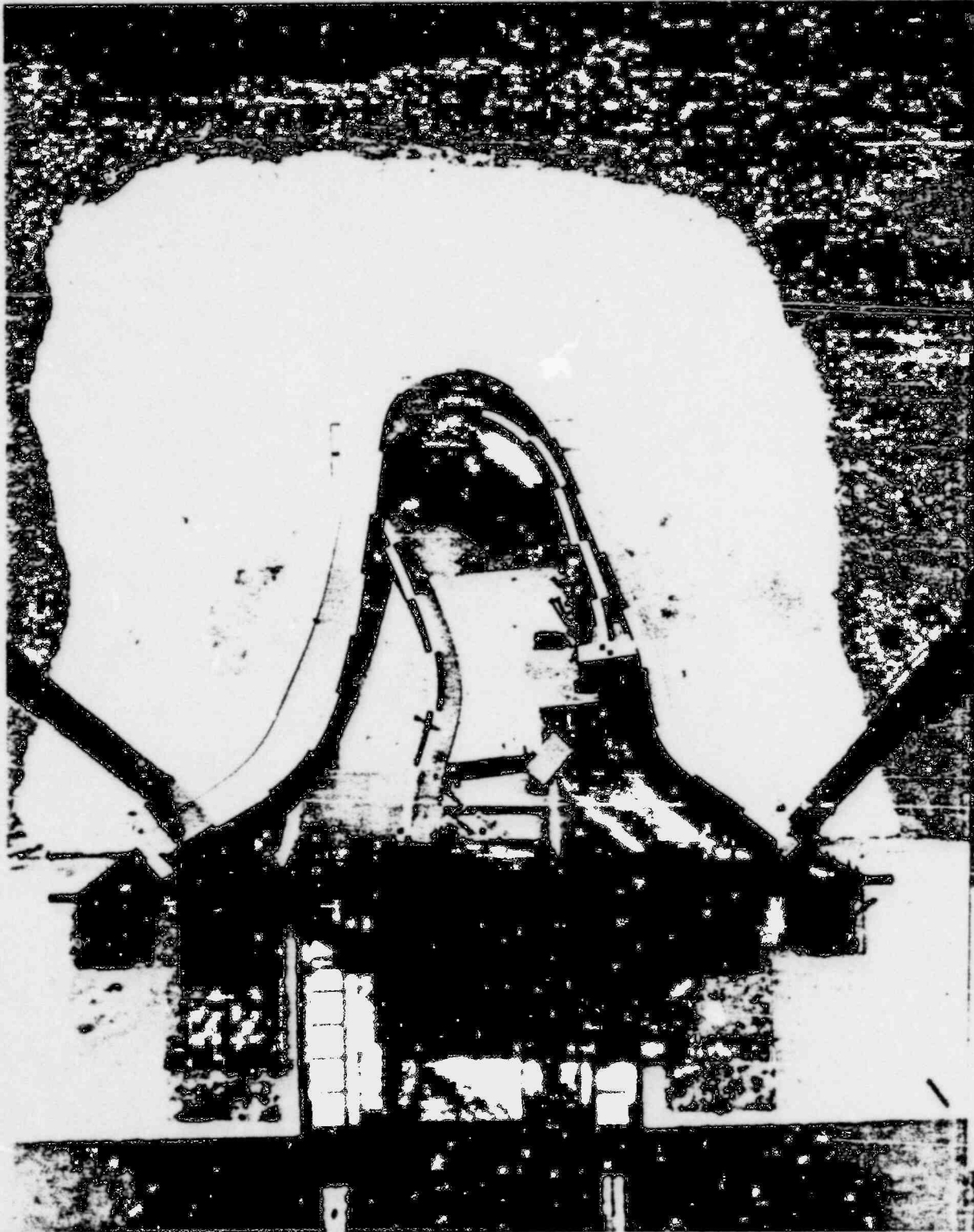


Figure 2-5c. Overhead photograph of blunt impact ($V = 8$ m/s, 25 ft/s; $\omega \approx 0$).

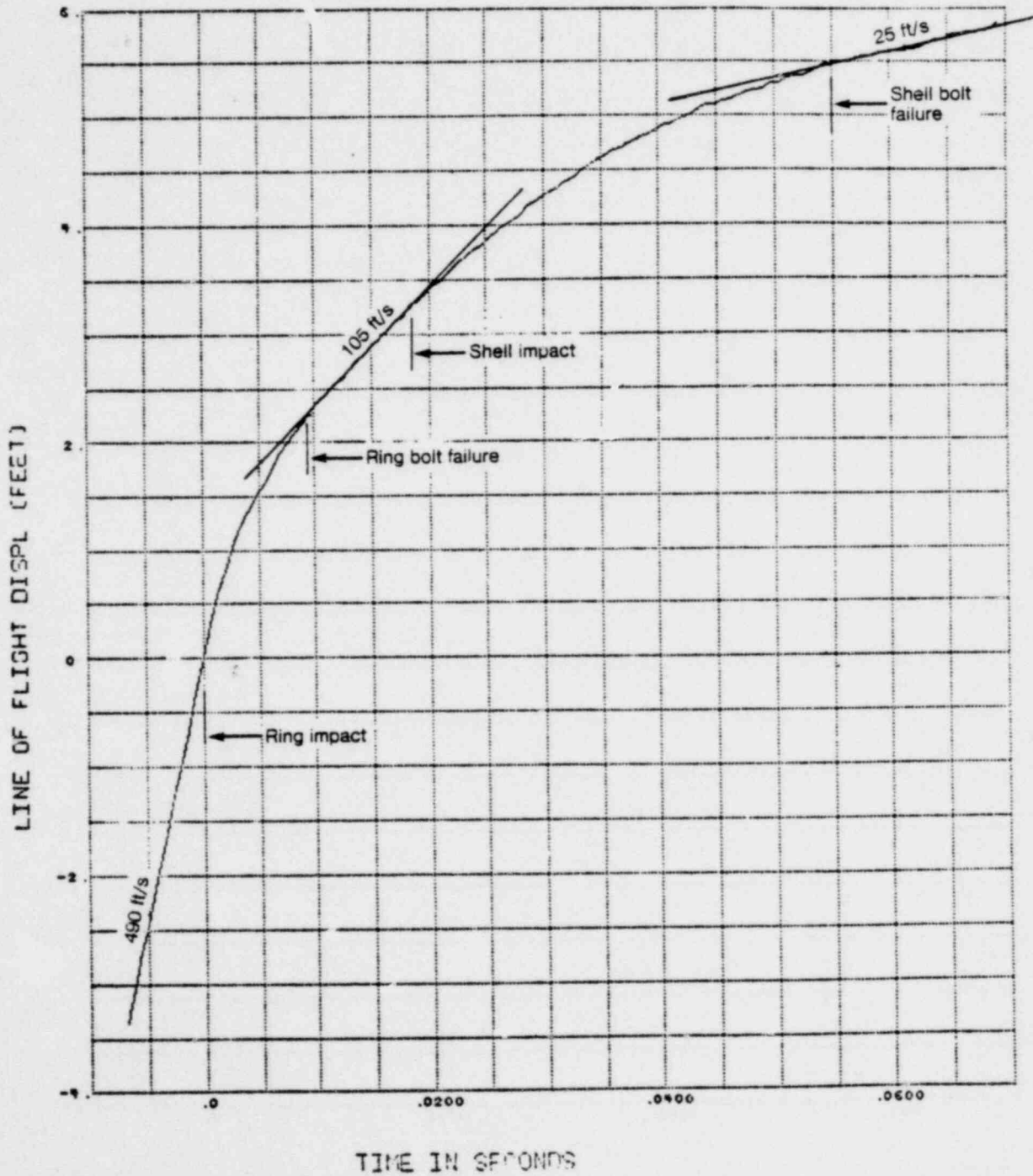


Figure 2-6. Displacement history of missile in test with blunt orientation
 (1 ft = 30.48 cm; 1 ft/s = 0.305 m/s)